JOC The Journal of Organic Chemistry

Article

pubs.acs.org/joc

Polyanils and Polyboranils: Synthesis, Optical Properties, and Aggregation-Induced Emission

Denis Frath, Karima Benelhadj, Maxime Munch, Julien Massue,* and Gilles Ulrich*

Institut de chimie et procédés pour l'énergie, l'environnement et la santé (ICPEES), groupe Chimie Organique pour les Matériaux, la Biologie et l'Optique (COMBO), UMR CNRS 7515, Ecole Européenne de Chimie, Polymères et Matériaux (ECPM), 25 Rue Becquerel, Strasbourg 67087 Cedex 2, France

Supporting Information

ABSTRACT: A first series of polyanils were synthesized by a simple condensation between either isomers of phenylenediamine derivatives or 1,3,5-benzenetriamine and 4-(diethylamino)salicylaldehyde, while a second series resulted from the condensation between 4,6-dihydroxyisophthalaldehyde or 2,5-dihydroxyterephthalaldehyde and differently substituted anilines. All these polyanils showed good chelating abilities toward trivalent boron fragments such as BF_2 or BPh_2 to yield the corresponding boranils. The optical properties of these novel fluorophores have been studied both in solution and in the solid-state and show emission wavelengths covering the entire visible spectrum and near-infrared (NIR), depending on molecular structure, substitution, and environment. While faintly fluorescent in solution in their molecular state, some polyanils show typical aggregation-induced emission (AIE) behavior upon addition of increasing amounts of water in THF solution, leading to a sizable enhancement of fluorescence intensity.

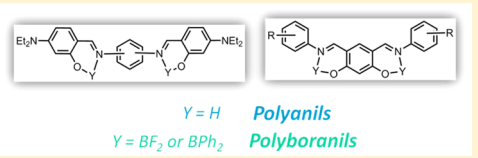

INTRODUCTION

Recent literature reports attest to the continuing effort devoted to the development of innovative organic luminescent fluorophores[1] for a wide range of applications in the biotechnologies field, from bioimaging contrast agents[2] to molecular sensors,[3] or in optoelectronic devices such as photovoltaic cells[4] or electroluminescent devices.[5]

Among all synthetic fluorophores studied, very promising features, such as high quantum yields, fine-tuned absorption/emission wavelengths, and photostability, have been observed for boron complexes of π-conjugated chelates. This family of dyes includes notably the legendary boron dipyrromethene (BODIPY) family[6] but also more recent analogues[7] based on N^O,[8] N^N[9] or N^C[10] chelates. In this context, a new family of fluorescent boron complexes, so-called boranils, was recently introduced, built around an N^B^O pattern, using anil (aniline−imine, also called salicylaldimine) ligands.[11] The fluorescence emission of anils in solution is usually very weak due to detrimental intramolecular rotations and/or isomerization upon irradiation.[7,11,12] Nevertheless, several examples of salicylaldimine[13] or salicyladehyde azines[14] have been described to brighten in the aggregated state due to beneficial aggregation-induced emission (AIE)[15] owing to a sizable restriction of intramolecular rotations.[16] AIE fluorogens are attractive platforms for bioimaging along with various biomedical applications.[17] Boranils are intrinsically much more fluorescent in the molecular state than their ligands counterparts due to a beneficial structural rigidification induced by the presence of the boron fragment.[12] Along with promising photophysical properties, boranil dyes are also interesting candidates for bioconjugation to proteins such as bovine albumin serum (BSA) in biological media.[18] Luminescent fluorophores containing several boron centers are often advantageous over isolated dyes because they seem to contribute to enhanced luminescence intensity, molar absorption coefficient, and overall brightness.[19] Additionally, functionalization of multiple boron fragments by sterically hindered substituents can prevent the formation of detrimental aggregates, leading to enhanced solid-state emission.[8c] Until now, very few examples of polyanils and polyboranils are reported in the literature.[20] In this paper, a series of original polyanils and polyboranils are described. They were synthesized in a one-step synthesis from salicylaldehyde and aniline derivatives, and the full optical characterization of these new fluorophores in solution and in the solid state was investigated. Additionally, some polyanils showed AIE behavior upon addition of increasing amounts of water in THF solution. These highly fluorescent aggregates were characterized by emission spectroscopy and dynamic light-scattering (DLS).

RESULTS AND DISCUSSION

The synthesis of polyanils **1**−**5** and polyboranils **6**−**10** is represented in Scheme 1, that of polyanils **12**−**13** and polyboranils **14**−**16** in Scheme 2, and that of polyanils **18**−**19** and polyboranils **20**−**21** in Scheme 3.

Polyanils **1**−**5** were synthesized in a one-step reaction by refluxing commercially available isomers of phenylenediamine and 4-(diethylamino)salicylaldehyde in absolute ethanol with trace amounts of *p*-TsOH (Scheme 1). Compounds **1**−**5** either precipitated pure from the medium or were purified by column chromatography on silica. Subsequent boron complexation was

Received: July 22, 2016
Published: October 3, 2016

DOI: 10.1021/acs.joc.6b01756
J. Org. Chem. 2016, 81, 9658−9668

Scheme 1. General Scheme for the Synthesis of Polyanils 1−5 and Their Corresponding Polyboranil Complexes 6−10

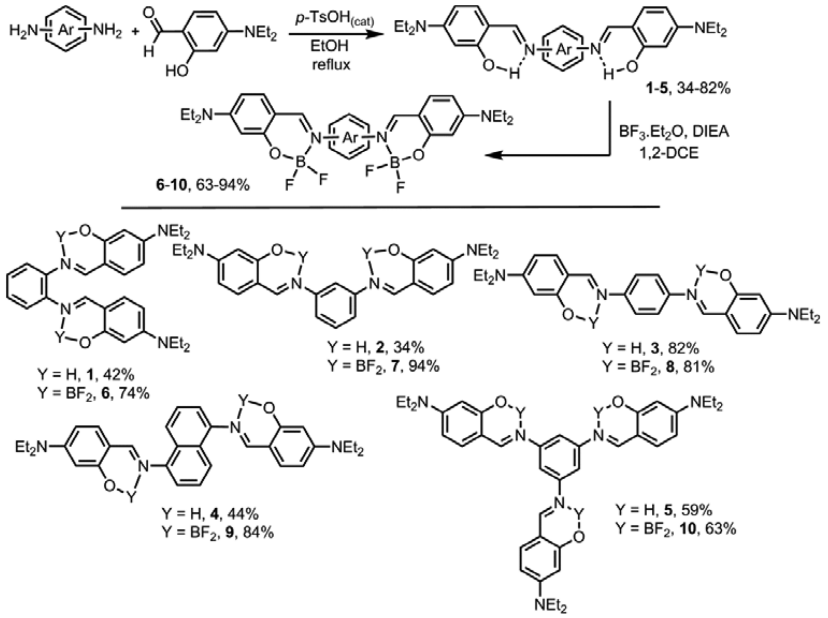

Scheme 2. General Scheme for the Synthesis of Polyanils 12−13 and Their Corresponding Polyboranil Complexes 14−16

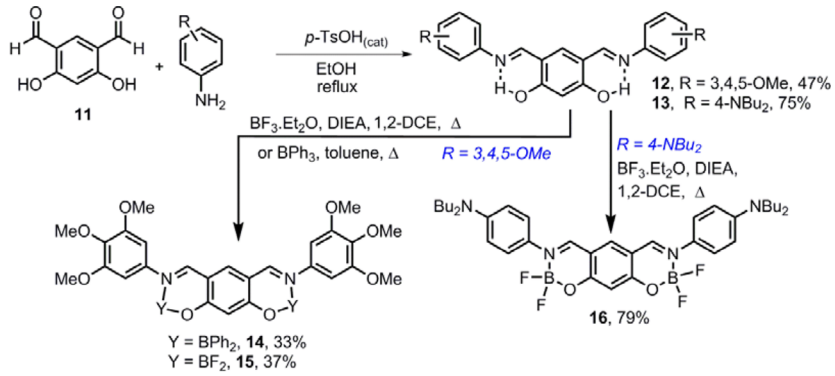

Scheme 3. General Scheme for the Synthesis of Polyanils 18−19 and Their Corresponding Polyboranil Complexes 20−21

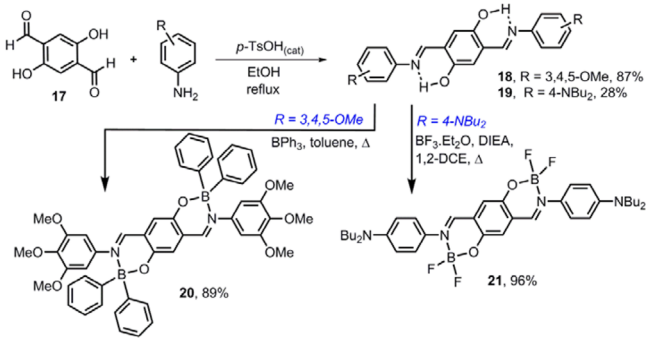

realized by the addition of a slight excess of $BF_3{\cdot}Et_2O$ on polyanils **1−5** in dry 1,2-dichloroethane under basic conditions (*N*,*N*-diisopropylethylamine (DIEA)). The complexation could be readily monitored by assessing the disappearance of the distinctive downfield signal corresponding to the H-bonded phenolic proton in ^{1}H NMR spectroscopy. Polyboranils **6−10** were purified by column chromatography on silica.

Polyanils **12−13** and **18−19** were obtained following a synthetic route similar to that of **1−5**, that is, by refluxing 4,6-dihydroxyisophthaldehyde **11**[21] (Scheme 2) or 2,5-dihydroxyterephthalaldehyde **17**[22] (Scheme 3) with the corresponding aniline derivative, i.e., 3,4,5-trimethoxyaniline or 4-amino-*N*,*N*-dibutylaniline[23] in absolute ethanol, followed by purification. The boron complexation was conducted in the same fashion as for polyboranils **6−10**, that is, reaction with an excess of $BF_3{\cdot}Et_2O$ in dry 1,2-dichloroethane in the presence of DIEA or with an excess of BPh_3 in toluene in the case of **14** and **20**, leading to polyboranils **14−15** and **20−21** after purification by column chromatography on silica gel.

All compounds were characterized by ^{1}H, ^{13}C NMR spectroscopy and HR-MS, reflecting their molecular structure in each case.

The aromatic regions of the ^{1}H NMR spectra of polyanil **19** and its corresponding borate complex **21** are presented in Figure 1. For polyanil **19**, a distinctive downfield peak corresponding to the H-bonded phenolic protons can be observed (δ = 13.12 ppm). Chelation to the B(III) fragment can be confirmed not only by assessing the disappearance of the phenolic peaks but also by acknowledging a shift of the peak corresponding to the aromatic protons close to the boron center. Furthermore, the imine protons, which are observed as

DOI: 10.1021/acs.joc.6b01756
J. Org. Chem. 2016, 81, 9658−9668

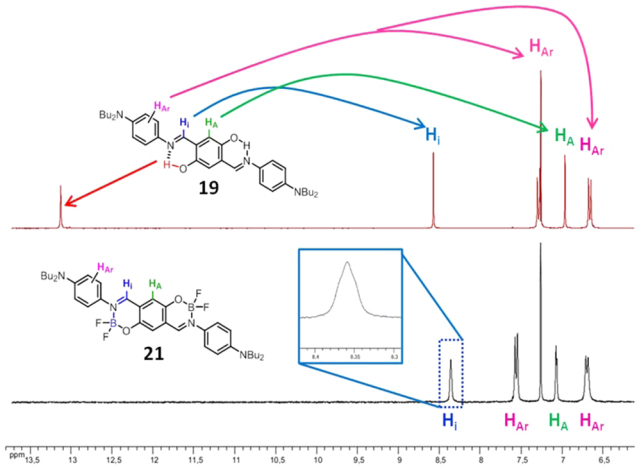

Figure 1. Aromatic regions of the ^{1}H NMR spectra of polyanil **19** (top) and polyboranil **21** (bottom) in $CDCl_3$ at room temperature.

a narrow singlet (δ = 8.57 ppm) in polyanil **19**, undergo a pronounced broadening upon complexation. The large singlet, which can be observed in the ^{1}H NMR spectrum of polyboranil **21**, corresponds to a sizable proton-B coupling between the imine proton and the boron atom, a feature already observed on related derivatives.[24]

All compounds have been additionally characterized by infrared spectroscopy where they all display a typical stretching band in the range 1610−1630 cm^{-1}, characteristic of the C═N imine elongation. Depending on their molecular structures, all dyes investigated display additional C═C and C−H stretching bands in the expected ranges.

Photophysical properties of polyanils **1**−**5**, **12**−**13**, and **18**−**19** are shown in Table 1. Absorption spectra of polyanils **1**−**5**, **12**−**13**, and **18**−**19** in THF are presented in Figure 2a, while absorption, emission, and excitation spectra of polyanils **3** and **13** are presented in parts b and c, respectively, of Figure 2.

As a general trend, all polyanil dyes display similar absorption spectra, i.e., a large, unstructured absorption band located in the UV part of the spectrum between 355 and 436 nm. Additional bands are observed at higher energies and are attributed to the $\pi-\pi^*$ transitions of the phenyl rings. Molar absorption coefficients are in the range 21000 to 130100 $M^{-1}\cdot cm^{-1}$, which is consistent for polyaromatic dyes. Polyanil **5**, whose structure comprises of three anil units connected onto a phenyl ring, displays the highest molar absorption coefficient in the series (130100 $M^{-1}\cdot cm^{-1}$) while maintaining its maximum absorption wavelength in the UV (λ_{abs} = 393 nm).

Polyanil **19** stands out in the polyanil series since it displays a significant red-shifted maximum absorption wavelength (λ_{abs} = 506 nm) compared to other polyanils along with a high molar absorption coefficient of 75800 $M^{-1}\cdot cm^{-1}$. The structured shape of the absorption band of **19** in THF is characteristic of a merocyanine-type molecular skeleton.

None of the polyanil dyes studied herein display a sizable fluorescence in solution in THF with the notable exception of polyanils **3** and **13** (Figures 2b,c). Upon excitation in the lowest energy absorption band, **3** and **13** display an intense emission band whose wavelength peaks at 500 and 606 nm, respectively, with a quantum yield calculated to be 10 and 3%, respectively. In both cases, the excitation spectrum matches the absorption one precluding the presence of emissive aggregates in the excited state and ascertaining the molecular species as the sole emitter. The para conformation of polyanil **3** tends to decrease nonradiative deactivations in the excited state, leading to a sizable green emission, as compared to its nonfluorescent isomeric analogues. In the case of **13**, the meta conformation seems to be beneficial for a decrease of the ICT phenomenom, as compared to the full quenched polyanil **19**, which displays a para conformation.

Photophysical data of polyboranils **6**−**10**, **14**−**16**, and **20**−**21** recorded in solution in various solvents are collected in Table 1, and their absorption and emission spectra recorded in dichloromethane are displayed in Figures 3 and 4 respectively.

The absorption spectra of all polyboranils compounds, with the notable exception of **21** display similar optical features such a broad, unstructured band, a maximum wavelength comprised between 370 and 433 nm and molar absorption coefficients ranging from 13100 and 188300 $M^{-1}\cdot cm^{-1}$ (Figure 3). The absence of structuration of the absorption bands is presumably related to free rotations occurring in solution. Those features are very similar to those observed for their polyanils analogues, such as a very high molar absorption coefficient (ε = 188300 $M^{-1}\cdot cm^{-1}$) for dye **10**, which incorporates three anil moieties. Polyboranil **21**, which displays a quadripolar donor−acceptor−donor molecular structure, exhibits a maximum absorption wavelength that is strongly bathochromically shifted as compared to other polyboranils (λ_{abs} = 589 nm in dichloromethane for **21** vs λ_{abs} = 370−433 nm for **6**−**10**, **14**−**15**, and **20**). Moreover, unlike other polyboranil derivatives, the maximum absorption wavelength of compound **21** seems to be dependent on the dipole moment of the solvent. Indeed, as the polarity of the solvent increases, the maximum absorption wavelength of **21** undergoes a significant hypsochromic shift (λ_{abs} = 594 nm in toluene to λ_{abs} = 473 nm in ethanol). This reported phenomenon, called inverted solvatochromism,[25] highlights the presence of a sizable dipole moment in the ground state.

The emission properties of all polyboranils were tested in a range of solvents with increasing dipole moment in order to investigate their solvatochromic properties in the excited state. Solubility issues impeded their complete study, but dichloromethane was found to be suitable for comparative studies (Figure 4).

In dichloromethane, excitation in the lowest energy absorption band led to the appearance of an emission band for polyboranils **7**−**10**, **14**, and **16**, while the fluorescence of polyboranils **6**, **15**, **20**, and **21** appeared to be fully quenched in solution. Depending on substitution, the maximum emission wavelength spanned from 457 to 609 nm with quantum yields up to 56% in dichloromethane. Interestingly, polyboranils **7** and **10** displayed similar optical properties (λ_{em} = 457 nm, Φ = 43% for **7** and λ_{em} = 460 nm, Φ = 49% for **10** in dichloromethane). In the case of dye **10**, the connection of an additional boranil fragment does not seem to have an influence on the optical properties of the resulting polychromophoric scaffold. Polyboranil **8** appears to be the brightest in the series with a quantum yield spanning from 56 to 90%. The most striking observation concerning dye **8** is that in polar solvent with a high dipole moment like acetonitrile the quantum yield remains high (Φ = 68%), as opposed to the general trend where a significant increase of nonradiative deactivations, detrimental to the quantum yield, is usually observed as the dipole moment of the solvent increases. The emission wavelength of polyboranils series **6**−**10** does not appear to be sensitive to the dielectric constant of the solvent, highlighting a probable cyanine-like

DOI: 10.1021/acs.joc.6b01756
J. Org. Chem. 2016, 81, 9658−9668

Table 1. Optical Data of Polyanils 1−5, 12−13, 18−19 and Polyboranils 6−10, 14−16, 20−21 Measured in Aerated Solution at Room Temperature

dye	λ_{abs}[a] (nm)	ε[b] ($M^{-1}\cdot cm^{-1}$)	λ_{em}[c] (nm)	ΔS[d] (cm^{-1})	Φ_F[e]	τ[f] (ns)	solvent	k_r[g]	k_{nr}[g]
1	355	62900	*h*	*h*	*h*	*h*	THF	*h*	*h*
2	389	82400	*h*	*h*	*h*	*h*	THF	*h*	*h*
3	416	76200	500	4000	0.10	0.08	THF	12.5	113.0
4	404	57800	*h*	*h*	*h*	*h*	THF	*h*	*h*
5	393	130100	*h*	*h*	*h*	*h*	THF	*h*	*h*
12	364	29500	*h*	*h*	*h*	*h*	THF	*h*	*h*
13	407	57800	606	8100	0.03	0.15	THF	2.0	64.7
18	436	21000	*h*	*h*	*h*	*h*	THF	*h*	*h*
19	506	75800	*h*	*h*	*h*	*h*	THF	*h*	*h*
6	374	71200	*h*	*h*	*h*	*h*	toluene	*h*	*h*
6	370	62200	*h*	*h*	*h*	*h*	CH_2Cl_2	*h*	*h*
7	417	110400	457	1800	0.43	0.9	CH_2Cl_2	4.8	6.3
7	416	112800	458	1800	0.01	1.2	CH_3CN	0.1	8.3
8	428	68000	506	3600	0.90	1.1	toluene	8.2	0.9
8	434	90000	510	3400	0.56	1.3	CH_2Cl_2	4.3	3.4
8	427	72100	507	3700	0.78	1.2	THF	6.5	1.8
8	427	66700	506	3700	0.68	1.1	CH_3CN	6.2	2.9
8	427	88300	504	3600	0.71	1.2	acetone	5.9	2.4
9	390	51500	485	4800	0.10	0.3	toluene	3.3	3.0
9	401	109600	474	3800	0.12	0.5	CH_2Cl_2	2.4	17.6
10	423	148700	460	1800	0.49	0.9	CH_2Cl_2	5.4	5.7
10	417	145000	463	2100	0.01	0.1	CH_3CN	1.0	99.0
10	419	188300	464	2300	0.04	0.1	acetone	4.0	96.0
14	391	31600	558	7700	0.09	0.5	toluene	1.8	18.2
14	376	33900	559	8400	0.06	0.5	CH_2Cl_2	1.2	18.8
15	418	29200	556	5900	0.04	0.2	toluene	2.0	48.0
15	381	31200	*h*	*h*	*h*	*h*	CH_2Cl_2	*h*	*h*
16	473	39400	571	3600	0.35	1.4	toluene	2.5	4.64
16	484	44000	609	4900	0.21	1.0	CH_2Cl_2	2.1	7.9
16	458	42700	635	6100	0.02	1.0	acetone	0.2	9.8
16	462	42200	620	5500	0.02	1.2	EtOH	0.2	8.2
20	433	13100	*h*	*h*	*h*	*h*	toluene	*h*	*h*
20	433	17300	*h*	*h*	*h*	*h*	CH_2Cl_2	*h*	*h*
21	594	49800	665	1700	0.31	1.6	toluene	1.9	4.3
21	589	51000	*h*	*h*	*h*	*h*	CH_2Cl_2	*h*	*h*
21	505	48200	*h*	*h*	*h*	*h*	acetone	*h*	*h*
21	473	55200	*h*	*h*	*h*	*h*	EtOH	*h*	*h*

[a]Maximum absorption wavelength. [b]Molar absorption coefficient. [c]Maximum emission wavelength. [d]Stokes' shift. [e]Quantum yield determined in solution by using quinine sulfate as a reference λ_{exc} = 366 nm, Φ = 0.55 in 1 N H_2SO_4 for dyes emitting below 480 nm, rhodamine 6G as a reference λ_{exc} = 488 nm, Φ = 0.88 in ethanol for dyes emitting between 480 and 570 nm, or cresyl violet λ_{exc} = 546 nm, Φ = 0.55 in ethanol as a reference for dyes emitting above 570 nm. [f]Lifetime. [g]k_r (10^8 s^{-1}) and k_{nr} (10^8 s^{-1}) were calculated using the following equations: $k_r = \Phi_F/\tau$, $k_{nr} = (1\ \Phi_F)/\tau$. [h]Nonfluorescent.

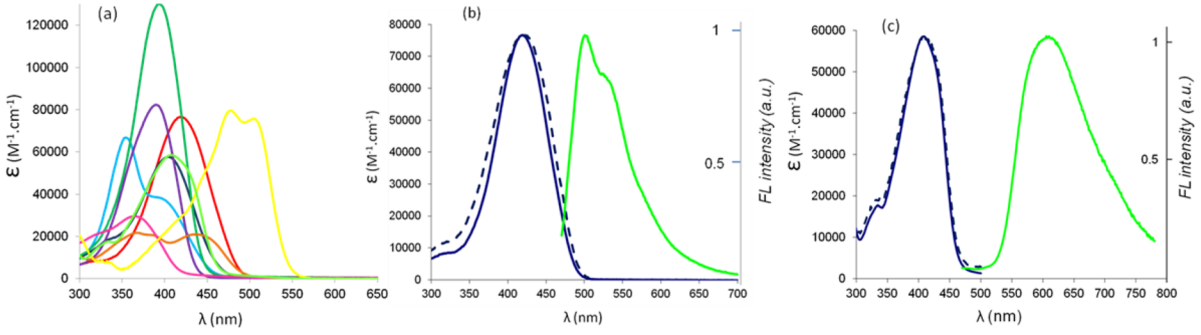

Figure 2. (a) UV−vis spectra recorded in THF at room temperature for polyanils **1** (blue), **2** (purple), **3** (red), **4** (dark blue), **5** (dark green), **12** (pink), **13** (light green), **18** (orange), and **19** (yellow). (b) Spectroscopic data for polyanil **3**: absorption (plain blue), excitation (detection at 515 nm, dashed blue) and emission (λ_{exc} = 490 nm, green). (c) Spectroscopic data for polyanil **13**: absorption (plain blue), excitation (detection at 625 nm, dashed blue), and emission (λ_{exc} = 400 nm, green).

DOI: 10.1021/acs.joc.6b01756
J. Org. Chem. 2016, 81, 9658−9668

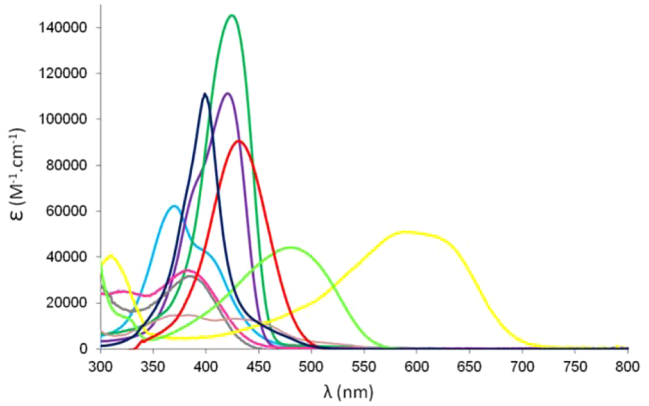

Figure 3. UV−vis spectra recorded in dichloromethane at room temperature for polyboranils **6** (blue), **7** (purple), **8** (red), **9** (dark blue), **10** (dark green), **14** (pink), **15** (gray), **16** (light green), **20** (orange), and **21** (yellow).

conformation in the excited state and a fluorescence emission presumably stemming from a singlet state. In the case of polyboranils **7** and **10**, the quantum yield decreases as the dielectric constant of the solvent increases,an indication of the probable presence of a low-lying nonemissive charge-transfer state.

Polyboranils **14** and **15** display the same 3,4,5-trimethoxy substitution and structure but differ by the nature of the boron fragment, i.e., BPh_2 for **14** and BF_2 for **15**. Introduction of a BPh_2 fragment does not seem to make a difference in terms of maximum emission wavelength (λ_{em} = 558 nm for **14** vs λ_{em} = 556 nm for **15** in toluene), which is in contrast with the general trend observed for other N^B^O borate complexes where substitution of a BF_2 group for a BPh_2 one induces a sizable red-shift in emission.[26,8c] The quantum yield is, however, higher in the case of **14** than for **15** (Φ = 9 and 4% respectively in toluene), evidencing a slight role of the sterically hindered phenyl rings in reducing nonradiative deactivations. Additionally, the beneficial introduction of BPh_2 is observed in dichloromethane where polyboranil **14** is found to be fluorescent (λ_{em} = 559 nm, Φ = 6%), which is not the case of **15**. Further optical studies in other solvents could not be conducted due to the lack of solubility of **14** and **15**. Polyboranils **14** and **20** feature, respectively, a 2,4- or a 2,5-disubstitution with respect to the position of the anil moieties. While, as described previously, dye **14** is mildly fluorescent in toluene or dichloromethane, the fluorescence emission of compound **20** in these two solvents was found to be completely quenched. This clearly shows that either the 2,5-disubstitution is not a good scaffold to provide a good conjugation between the boron centers and the methoxy substituents on the phenyl rings or that this molecular morphology likely leads to the detrimental formation of intermolecular aggregates. It is to be noted that attempts to prepare the BF_2 analogue of polyboranil **20** failed due to the lack of stability of the crude product obtained which could not undergo a purification step. Polyboranils **16** and **21** were found to be highly soluble in most solvents due to the beneficial presence of solubilizing butyl chains. In toluene, dye **21** displays a maximum emission wavelength, which is located in the red part of the spectrum and features a striking bathochromic shift as compared to the rest of the series (λ_{em} = 665 nm for **21** vs λ_{em} = 457−558 nm for other polyboranils in toluene). Another surprising feature is the value of the quantum yield, which remains high (Φ = 31%) for an emission located in such low energies. Polyboranil **16**, which displays the same electronic substituents but in a meta fashion, is blue-shifted in absorption and emission in toluene, as compared to **21** (λ_{abs} = 473 nm, λ_{em} = 571 nm, Φ = 35%). To

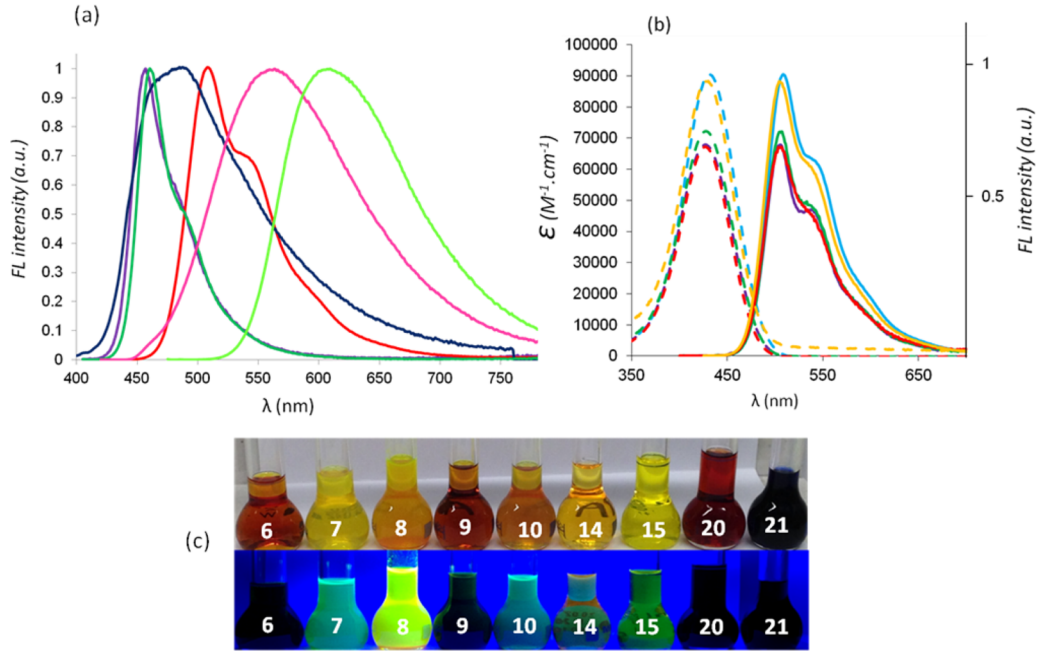

Figure 4. (a) Emission spectra of polyboranils **7** (λ_{exc} = 405 nm, purple), **8** (λ_{exc} = 415 nm, red), **9** (λ_{exc} = 390 nm, dark blue), **10** (λ_{exc} = 413 nm, dark green), **14** (λ_{exc} = 365 nm, pink) and **16** (λ_{exc} = 470 nm, light green) in dichloromethane at room temperature, (b) absorption (dashed) and emission (λ_{exc} = 415 nm, plain) of polyboranil **8** in toluene (purple), dichloromethane (blue), THF (green), acetone (orange), and acetonitrile (red), and (c) photographs of dicholoromethane solutions of polyboranils taken under ambient light (top) and under UV-bench lamp (λ_{exc} = 365 nm) (bottom).

DOI: 10.1021/acs.joc.6b01756
J. Org. Chem. 2016, 81, 9658−9668

investigate the solvatochromic nature of the emission band, the optical properties of **16** and **21** were studied in solvents of increasing dipole moment. While the absorption of **16** does not undergo any major change upon increase of the dipole moment of the solvent, the emission maximum wavelength spans from 571 to 635 nm depending on solvent with a significant decrease of the fluorescence quantum yield. Unfortunately, the emission of **21** was found to be completely quenched outside toluene, probably due to an important internal charge transfer (ICT) character of the emission.[27] To evidence the presence of a sizable ICT in **21**, protonation studies were conducted in the presence of HCl_{gas}, and the results in dichloromethane and acetone are shown in Figure 5.

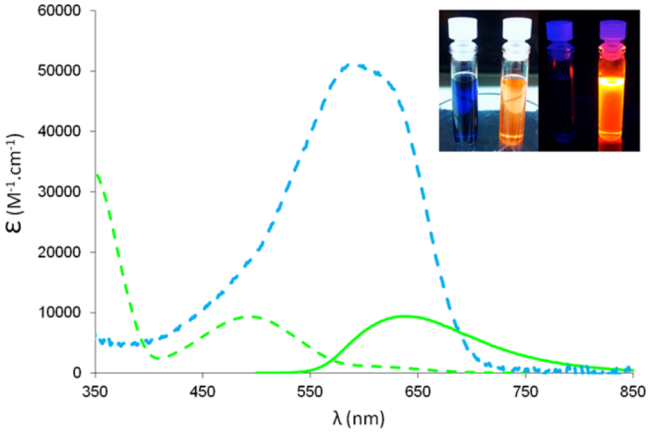

Figure 5. Absorption (dashed) and emission (λ_{exc} = 490 nm, plain) spectra of polyboranil **21** in dichloromethane in the neutral (blue) protonated state (green) at room temperature and (inset) photographs of polyboranils **21** in the neutral and protonated state in solution in dichloromethane under ambient light (left) and under UV-bench lamp (λ_{exc} = 365 nm) (right).

Protonation experiments were conducted by bubbling HCl_{gas} in a dichloromethane or acetone solution of **21**. First, upon protonation of the lone electron pair of the nitrogen atoms, maximum absorption wavelengths displayed a strong hypsochromic shift along with a hypochromic value of their molar absorption coefficient (λ_{abs} = 589 nm, ε = 51000 $M^{-1}\cdot cm^{-1}$ vs λ_{abs} = 495 nm, ε = 9400 $M^{-1}\cdot cm^{-1}$ for **21** in neutral and protonated dichloromethane, respectively, and λ_{abs} = 505 nm, ε = 48200 $M^{-1}\cdot cm^{-1}$ vs λ_{abs} = 466 nm, ε = 6800 $M^{-1}\cdot cm^{-1}$ for **21** in neutral and protonated acetone, respectively). This absorption change phenomenom has been previously observed for related borate complexes based on an isoquinoline framework.[28] Although completely quenched in dichloromethane and acetone in the neutral state, polyboranil **21** was found to sizably brighten up upon protonation. Indeed, excitation in the lowest energy absorption band led to the appearance of an intense emission band located in the orange in the case of the two solvents (λ_{em} = 640 nm, Φ = 24% in dichloromethane and λ_{em} = 620 nm, Φ = 5% in acetone). This is a clear indication that the emission in polyboranil **21** stems from an excited state with a strong ICT character. In the neutral state, a significant electronic delocalization occurs in the ground and excited state between the aromatic amine (donor) and the BF_2 fragment; **21** acts as a typical push−pull fluorophore.[29] This leads to a solvatochromic behavior in absorption. Upon protonation, the delocalization is no longer possible, making the ICT much weaker and leading to a hypsochromic shift in absorption and the appearance of a significant emission in dichloromethane and acetone. Protonation studies were also performed on polyboranil **16**, and the trends observed in **21** were similarly found (λ_{abs} = 484 nm, λ_{em} = 608 nm, Φ = 21% vs λ_{abs} = 380 nm, λ_{em} = 442 nm, Φ = 8% for **16** in neutral and protonated dichloromethane, respectively).

The emission properties of all polyanils and polyboranils were studied in the solid-state as embedded in KBr pellets (concentration around 10^{-6} M). The optical data are presented in Table 2, while the emission spectra of polyanils **2**−**5** and **13** and polyboranils **6**−**10**, **14**, **16**, and **20**−**21** are displayed in parts a and b, respectively, of Figure 6.

Table 2. Optical Data of Polyanils 2−5, 13 and Polyboranils 6−10, 14, 16, 20−21 Measured in the Solid State as KBr Pellets

dye	λ_{exc} (nm)	λ_{em} (nm)	ΔS (cm^{-1})	Φ_f [a]	x; y (CIE 1931)
2	476	548	2760	0.04	0.377; 0.420
3	512	554	1480	0.11	0.506; 0.474
4	484	514	1200	0.06	0.438; 0.388
5	498	591	3200	0.06	0.438; 0.384
13	556	644	2500	0.05	0.680; 0.325
6	465	601	4900	0.05	0.444; 0.395
7	489	525	1400	0.10	0.389; 0.473
8	529	560	1050	0.22	0.491; 0.436
9	487	588	3500	0.05	0.449; 0.381
10	474	534	2400	0.07	0.434; 0.405
14	443	541	4100	0.18	0.222; 0.455
16	576	642	1800	0.10	0.691; 0.309
20	550	720	4300	0.30	0.713; 0.288
21	692	789	1800	*b*	*b*

[a]Absolute quantum yield, calculated with an integrating sphere. [b]The emission of polyboranil **21** is located in the near-infrared (NIR), and the quantum yield cannot be accurately calculated with our current spectrophotometer.

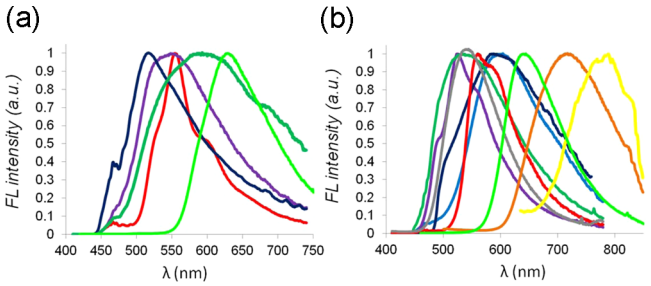

Figure 6. Emission (λ_{exc} = 400 nm) spectra recorded in the solid state in KBr pellets of (a) polyanils **2** (purple), **3** (red), **4** (dark blue), **5** (dark green), and **13** (light green) and (b) polyboranils **6** (blue), **7** (purple), **8** (red), **9** (dark blue), **10** (green), **14** (gray), **16** (light green), **20** (orange), and **21** (yellow).

As a general observation, the emission profiles for all studied compounds follow the same trends as those observed in the solution state, i.e., broad, unstructured emission bands covering most of the visible spectrum depending on substitution, except for para-substituted derivatives **3** and **8** comprising a cyanine-like structure, which display a relatively structured emission band.

First, it is to be noted that polyanils **2**, **4**, and **5** are slightly emissive in the solid state, whereas they were fully quenched in solution in THF (λ_{em} = 514−591 nm) (Figure 6a). The

DOI: 10.1021/acs.joc.6b01756
J. Org. Chem. 2016, 81, 9658−9668

quantum yields, calculated with a spectrofluorimeter fitted with an integration sphere, are in the range 4−6%. Polyanil **3** exhibits a structured emission band with a maximum wavelength at 554 nm and a quantum yield of 11%, which corresponds to a significant red-shift as compared to its emission profile in solution (λ_{em} = 500 nm, Φ = 10% in THF). Embedment in a confined matrix seems to be beneficial for the sizable decrease of nonradiative deactivations due to the restriction of molecular rotations and torsions. Similar conclusions can be drawn for polyboranils **6** and **20** whose fluorescence was switched off in solution but fully on in the solid state (λ_{em} = 601 nm, Φ = 5% and λ_{em} = 720 nm, Φ = 30% for **6** and **20**, respectively). This observation is especially striking for polyboranil **20**, which displays in the solid state an emission band located in the far-red region with a strong quantum yield of 30%, a value rarely calculated for such small energy radiations. This is particularly interesting owing to the broad number of applications arising from bright solid-state emitters.[30]

Polyboranils **7**−**10** and **21** which were already fluorescent in solution all undergo a bathochromic shift in solid-state emission that is more or less pronounced depending on substitution. Polyboranils dyes **7**−**10** display an emission wavelength in the visible region in the range 525−588 nm, while **21** exhibits an emission wavelength in the near-infrared (NIR) region at 789 nm. Polyboranil **14** is the only dye in the series to exhibit a slight blue-shift upon insertion in a solid matrix (λ_{em} = 541 nm, Φ = 18%).

Recent publications report the AIE behavior of related functionalized anil derivatives in mixtures of solvent[15] which prompted us to examine the aggregation ability of the various polyanils dyes developed in our study and evaluate their potential use as multicolor fluorogens.

First, the AIE behavior of the polyanil derivatives **1**, **2**, **4**, and **5** were tested by adding increasing amounts of water (water fraction, named f_w from 0% to 98%), buffered by PBS (0.1 M) at pH 7.4. These polyanils dyes were not fluorescent in THF solution. In the aggregated state, excitation at 400 nm led to the appearance of a sizable emission of light at a maximum wavelength of 528 nm in the case of **2** and **5** at a concentration of 50 μM. Polyanils **1** and **4** did not display detectable AIE behavior. The emission spectra of **2** and **5** are displayed in parts a and b, respectively, of Figure 7.

As shown in Figure 7a,b, dyes **2** and **5** were not fluorescent in pure THF solution, and the emission intensity, monitored at 528 nm, did not show any increase before f_w reached 60% and 40% for **2** and **5**, respectively. At this point, the intensity at 528 nm started to rise steeply to reach a maximum value of f_w 98%. This intensity enhancement represents a 25-fold and 46-fold increase for polyanils **2** and **5**, respectively, from THF solution to the 98% aqueous mixture.

Then, similar AIE experiments were carried out on polyanil **3** which already displays fluorescence in THF solution (λ_{em} = 500 nm, Φ = 10%). The emission spectra recorded upon increase of f_w along with the evolution of the intensity of the emission band at 552 nm are collected in Figure 8.

Addition of increasing amounts of water leads to the appearance of an additional emission band at a longer wavelength compared to that observed in pure THF (λ_{em} = 552 nm vs λ_{em} = 500 nm in THF). The intensity at 552 nm first started to rise softly up to f_w 40%, leading to a dual emission at 500 and 552 nm, corresponding to the presence of **3** in the molecular and the aggregated state, respectively. Upon further

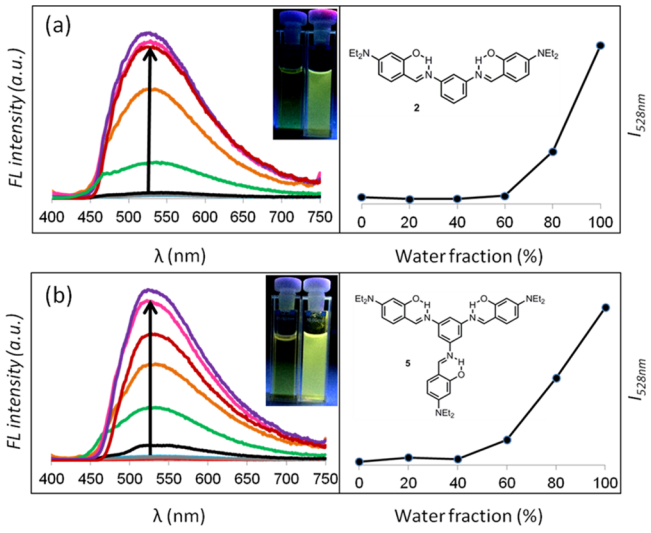

Figure 7. (Left) Fluorescence emission spectra in THF with different water fraction at pH 7.4 buffered by PBS 0.1 M. (Right) Fluorescence emission peak intensity at 528 nm as a function of water fraction for (a) polyanil **2** and (b) polyanil **5**. Polyanils were excited at 400 nm. Photographs were taken under UV light at 365 nm.

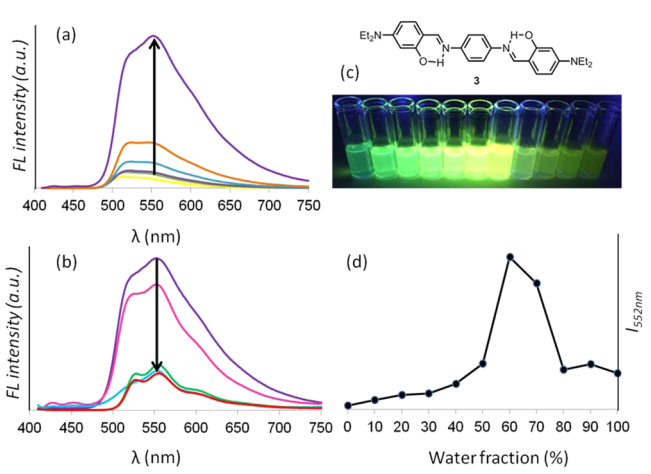

Figure 8. (a) Fluorescence emission spectra in THF with water fraction from 0 to 60% at pH 7.4 buffered by PBS 0.1 M, (b) fluorescence emission spectra in THF with water fraction from 60 to 100% at pH 7.4 buffered by PBS 0.1 M, (c) photographs of solutions of 3 in THF/PBS with water fraction from 0 to 100% (left to right) taken under UV light at 365 nm, and (d) fluorescence emission peak intensity at 552 nm as a function of water fraction for polyanil **3**. Excitation was 400 nm.

increase of f_w, a steep enhancement up to f_w 60% can be evidenced in the f_w/intensity at 552 nm plot. From that point on, the intensity was observed to decrease rapidly down to f_w 80% before reaching a plateau between f_w 80% and 98%. This AIE behavior is in strong contrast to typical AIE behavior observed for **2**, **5**, or related probes[13] where the fluorescence intensity gradually increases along with f_w. The intensity enhancement represented a 42-fold increase at 60% aqueous mixture before dropping to an 11-fold increase at 80%.

To shed more light on the nature of these aggregates, dynamic light-scattering (DLS) experiments were conducted for polyanils **2** and **5** in 98% aqueous solution and for polyanil **3** in 60% and 98% aqueous solutions. For each dye, DLS measurements were repeated 10 times, each time comprising

DOI: 10.1021/acs.joc.6b01756
J. Org. Chem. 2016, 81, 9658−9668

10 scans, and average results are reported in Figures S3−S6. For polyanils **2** and **5**, aggregates with an average size of 150 and 75 nm, respectively, were measured in 98% aqueous solutions. It is to be noted that these aggregates are stable over time in solution, and no dissociation could be observed after 48 h. For polyanil **3**, in a 60/40 THF/water mixture, DLS experiments revealed a particle size of the aggregates in the range 100−300 nm, consisting of previously reported literature probes.[13c] Additional particles are observed in the nanometer range, probably corresponding to the molecular species still present in solution, as evidenced by the presence of the emission band at 500 nm at f_w 60%. Upon an increase of f_w to 98%, the size distribution evolved largely toward the presence of both larger aggregates in the micrometer range and smaller particles evidencing a sizable dissociation of the aggregates. This hypothesis is also supported by the steep decrease of the intensity at 552 nm upon the increase of f_w.

In conclusion, two series of polyanils were constructed in a one-step synthesis from salicyladehydes and anilines followed by a boron complexation to form the polyboranils. Polyboranil dyes display sizable emission properties in solution and in the solid state, covering the entire visible spectrum and even reaching NIR in the condensed matter. Polyanils are faintly fluorescent in solution but display interesting AIE behaviors in THF/water solutions. In the aggregated state, up to a 46-fold enhancement of the intensity was observed. Structural modifications such as extension of conjugation are currently under investigation to target red-shifted aggregates and evaluate their role as biological probes.

EXPERIMENTAL SECTION

All reactions were performed under a dry atmosphere of argon using standard Schlenk techniques. All chemicals were received from commercial sources and used without further purification. Dichloromethane and 1,2-dichloroethane were distilled over P_2O_5 under an argon atmosphere. TLC was performed on silica gel coated with fluorescent indicator. Chromatographic purifications were conducted using 40−63 μm silica gel. All mixtures of solvents are given in a v/v ratio.

^{1}H NMR (400.1 MHz) and ^{13}C NMR (100.5 MHz) spectra were recorded on a 400 MHz spectrometer, ^{1}H NMR (300.1 MHz) and ^{13}C NMR (75.5 MHz) or a 300 MHz spectrometer with perdeuterated solvents with residual protonated solvent signals as internal references.

HRMS data were recorded on a microTOF spectrometer equipped with ESI.

Absorption spectra were recorded using a dual-beam grating absorption spectrometer with a 1 cm quartz cell. The steady-state fluorescence emission and excitation spectra were obtained by using a fluorimeter. Solvents for spectroscopy were spectroscopic grade and were used as received. All fluorescence spectra were corrected.

The fluorescence quantum yield (Φ_{exp}) was calculated from eq 1:

$$\Phi_{exp} = \Phi_{ref}\frac{I}{I_{ref}}\frac{f}{f_{ref}}\frac{\eta^2}{\eta_{ref}^2} \quad (1)$$

I denotes the integral of the corrected emission spectrum, f is the absorption factor at the excitation wavelength, and η is the refractive index of the medium. The quantum yield is determined in solution by using quinine sulfate as a reference λ_{exc} = 366 nm, Φ = 0.55 in 1 N H_2SO_4, for dyes emitting below 480 nm, Rhodamine 6G as a reference λ_{exc} = 488 nm, Φ = 0.88 in ethanol, for dyes emitting between 480 and 570 nm or cresyl violet λ_{exc} = 546 nm, Φ = 0.55 in ethanol as a reference for dyes emitting above 570 nm. The reference quantum yields were obtained using reported procedures.[31]

Solid-state absolute quantum yields were determined using an integrating sphere.[32] Luminescence lifetimes were measured on a spectrofluorimeter equipped with a R928 photomultiplier and a pulsed diode connected to a delay generator. No filter was used for the excitation. Emission wavelengths were selected by a monochromator. Lifetimes were deconvoluted with FS-900 software using a light-scattering solution for instrument response. The excitation source was a laser diode (λ_{exc} = 320 nm). IR spectra of were recorded on neat products (powder samples) using an ATR diamond plate. 4,6-Dihydroxyisophthaldehyde **11**,[20] 2,5-dihydroxyterephthalaldehyde **17**,[21] 4-Amino-N,N-dibutylaniline,[22] polyanil **1**,[33] polyanil **2**,[34] polyanil **3**[11a] and polyboranil **8**[11a] were synthesized according to reported procedures.

General Procedure I for the Synthesis of Polyanils 1−5, 12−13, and 18−19. To a solution of 0.2 mmol of the relevant di- or trianiline in 20 mL of dry ethanol was added the corresponding salicylaldehyde (0.4 mmol, 2 equiv) as a powder. *p*-TsOH (one crystal) was then added to the mixture, and the resulting solution was refluxed overnight. After the solution was cooled, either a precipitate appeared that was collected, further washed with ethanol and pentane, and dried under vacuum or purification was performed by column chromatography on silica using CH_2Cl_2 as eluent to yield the desired polyanils **1−5**, **12−13**, and **18−19** as yellow to red powders (28 to 87% yield).

Polyanil ***4***.[35] General procedure I was followed leading to **4** as a yellow crystalline powder 44% (45 mg). Mp: 290 °C dec. ^{1}H NMR (300 MHz, $CDCl_3$) δ (ppm): 13.85 (1H, s), 8.49 (1H, s), 8.17 (2H, d, ^3J = 8.3 Hz), 7.52 (2H, t, ^3J = 7.3 Hz), 7.22 (4H, m), 6.30 (4H, m), 3.44 (8H, q, ^3J = 7.3 Hz), 1.24 (12H, t, ^3J = 7.3 Hz). ESI-HRMS: calcd for $C_{32}H_{37}N_4O_2$ 509.2911 (M + H), found 509.2941 (M + H). IR (ν, cm^{-1}): 1620.8, 1581.5, 1515.2, 1447.9, 1425.3, 1391.4, 1374.1, 1344.3, 1305.2, 1235.8, 1219.6, 1191.1, 1075.7, 934.5, 821.3, 779.8.

Polyanil ***5***. General procedure I was followed leading to **5** as a yellow crystalline powder in 59% yield (77 mg). Mp: 240 °C. ^{1}H NMR (300 MHz, acetone-d_6) δ (ppm): 13.47 (3H, s), 8.79 (3H, s), 7.34 (3H, d, ^3J = 9.1 Hz), 7.12 (3H, s), 6.37 (3H, dd, ^3J = 9.1 Hz, ^4J = 2.4 Hz), 6.15 (3H, d, ^4J = 2.4 Hz), 3.48 (12H, q, J = 7.3 Hz), 1.20 (18H, t, J = 7.3 Hz); ^{13}C NMR (75 MHz, $CDCl_3$) δ (ppm): 164.6, 161.0, 152.2, 150.8, 134.2, 110.5, 109.3, 104.1, 98.0, 44.8, 12.9. ESI-HRMS: calcd for $C_{39}H_{49}N_6O_3$ 649.3861 (M + H), found 649.3884 (M + H). IR (ν, cm^{-1}): 1625.7, 1564.2, 1513.6, 1416.9, 1340.8, 1239.1, 1124.8, 1076.8, 785.6.

Polyanil ***12***. General procedure I was followed leading to **12** as a yellow crystalline powder in 47% yield (47 mg). Mp: 268−270 °C. ^{1}H NMR (400 MHz, $CDCl_3$) δ (ppm) = 14.12 (s, 2H), 8.79 (br s, 2H), 7.45 (s, 1H), 6.57 (s, 1H), 6.51 (s, 4H), 3.91 (s, 12H), 3.87 (s, 6H). ^{13}C NMR (75 MHz, $CDCl_3$) δ (ppm) = 166.5, 160.2, 154.0, 144.0, 137.8, 113.2, 104.6, 98.6, 92.9, 61.2, 56.4. ESI-HRMS: calcd for $C_{26}H_{29}N_2O_8$ 497.1918 (M + H), found 497.1950 (M + H). IR (ν, cm^{-1}): 1624.5, 1578.9, 1499.8, 1459.7, 1415.7, 1362.1, 1228.1, 1178.3, 1127.6, 992.6, 837.5, 815.2, 794.6.

Polyanil ***13***. General procedure I was followed leading to **13** as a red amorphous powder in 75% yield (76 mg). ^{1}H NMR (400 MHz, $CDCl_3$) δ (ppm) = 14.82 (s, 2H), 8.50 (s, 2H), 7.30 (s, 1H), 7.22 (d, 4H, ^3J = 9.2 Hz), 6.66 (d, 4H, ^3J = 8.8 Hz), 6.50 (s, 1H), 3.30 (t, 8H, ^3J = 7.2 Hz), 1.58−1.63 (m, 8H), 1.33−1.42 (m, 8H), 0.97 (t, 12H, ^3J = 7.6 Hz). ^{13}C NMR (75 MHz, $CDCl_3$) δ (ppm) = 166.2, 155.5, 147.4, 135.7, 135.2, 122.0, 113.3, 112.0, 104.4, 51.0, 29.5, 20.4, 14.0. ESI-HRMS: calcd for $C_{36}H_{51}N_4O_2$, 571.4007 (M + H), found 571.3955 (M + H). IR (ν, cm^{-1}): 1621.7, 1604.2, 1512.5, 1397.0, 1360.0, 1283.9, 1220.8, 1179.2, 1153.2, 1109.6, 926.4, 877.4, 842.9, 809.0, 798.1, 732.7, 528.3.

Polyanil ***18***. General procedure I was followed leading to **18** as a yellow crystalline powder in 87% yield (86 mg). Mp: 252 °C. ^{1}H NMR (400 MHz, $CDCl_3$) δ (ppm) = 12.59 (br s, 2H), 8.63 (s, 2H), 7.14 (s, 2H), 6.59 (s, 4H), 3.93 (s, 12H), 3.89 (s, 6H). ^{13}C NMR (100 MHz, $CDCl_3$) δ (ppm) = 161.0, 154.0, 153.1, 144.1, 137.9, 122.5, 119.3, 98.8, 61.2, 56.4. ESI-HRMS: calcd for $C_{26}H_{29}N_2O_8$, 497.1918 (M + H), found 497.1940 (M + H). IR (ν, cm^{-1}): 1586.0, 1502.3, 1467.3, 1327.1, 1232.3, 1163.4, 1131.5, 1002.8, 991.0, 824.6, 783.2, 642.8, 625.1.

DOI: 10.1021/acs.joc.6b01756
J. Org. Chem. 2016, 81, 9658−9668

Polyanil ***19***. General procedure I was followed leading to **19** as a red crystalline powder in 28% yield (32 mg). Mp: 127−128 °C. ^{1}H NMR (300 MHz, $CDCl_3$) δ (ppm) = 13.13 (s, 2H), 8.57 (s, 2H), 7.28 (d, 4H, ^3J = 9.0 Hz), 6.96 (s, 2H), 6.66 (d, 4H, ^3J = 9.0 Hz), 3.33−3.28 (t, 8H, ^3J = 7.5 Hz), 1.65−1.57 (m, 8H), 1.44−1.31 (m, 8H), 0.97 (t, 12H, ^3J = 7.3 Hz). ^{13}C NMR (75.5 MHz, $CDCl_3$) δ (ppm) = 155.6, 152.9, 148.1, 135.9, 122.8, 122.4, 118.1, 112.1, 51.1, 29.6, 20.5, 14.2. ESI-HRMS: calcd for $C_{36}H_{51}N_4O_2$, 571.4007 (M + H), found 571.3981 (M + H). IR (ν, cm^{-1}): 1609.1, 1572.9, 1501.4, 1366.5, 1349.0, 1333.5, 1314.7, 1211.4, 1172.9, 1155.4, 925.3, 879.2, 854.0, 812.5, 787.0, 523.6.

General Procedure II for the Synthesis of Polyboranils 6−10, 15, 16, and 21. To a stirred solution of 0.2 mmol of the relevant polyanil **1**−**5**, **12**−**13**, or **19** in 20 mL of distilled 1,2-dichloroethane at 85 °C was added $BF_3{\cdot}OEt_2$ (0.5 mmol, 2.5 equiv). A color change immediately occurred, or a precipitate appeared, revealing the formation of an in situ intermediary. *N*,*N*-Diisopropylethylamine (DIEA) (0.5 mmol, 2.5 equiv) was then added dropwise to the medium, and the course of the reaction was monitored by TLC analysis. After cooling, the reaction mixture was washed with a saturated solution of $NaHCO_3$ and extracted with dichloromethane three times. The organic layers were dried over $MgSO_4$, and the solvents evaporated in vacuo. Polyboranils **6**−**10**, **15**−**16**, and **21** were purified by silica or alumina gel chromatography (using CH_2Cl_2/petroleum ether 1:1 and CH_2Cl_2 as eluent, respectively) and obtained pure as yellow to purple powders (37−96% yield).

Polyboranil ***6***. General procedure II was followed leading to **6** as a yellow crystalline powder in 74% yield (82 mg). Mp: 253 °C. ^{1}H NMR (300 MHz, $CDCl_3$) δ (ppm): 8.09 (2H, br s), 7.65 (2H, m), 7.40 (2H, m), 7.13 (2H, d, ^3J = 9.1 Hz), 6.24 (2H, dd, ^3J = 9.1 Hz, ^4J = 2.2 Hz), 6.12 (2H, d, ^4J = 2.2 Hz), 3.38 (8H, q, J = 6.9 Hz), 1.18 (12H, t, J = 6.9 Hz); ^{13}C NMR (75.5 MHz, $CDCl_3$) δ (ppm): 163.5, 162.0, 156.7, 138.3, 135.0, 128.7, 128.4, 106.8, 98.1, 45.3, 12.9). ESI-HRMS: calcd for $C_{28}H_{33}B_2F_4N_4O_2$, 555.2730 (M + H), found 555.2728 (M + H). IR (ν, cm^{-1}): 1628.1, 1606.6, 1583.0, 1445.1, 1350.0, 1223.3, 1190.0, 1072.0, 1039.7, 973.4, 821.4, 791.4, 526.9.

Polyboranil ***7***. General procedure II was followed leading to **7** as a yellow crystalline powder in 94% yield (104 mg). Mp: 282−285 °C. ^{1}H NMR (300 MHz, $CDCl_3$) δ (ppm): 8.10 (2H, s), 7.53 (4H, m), 7.28 (2H, m), 6.39 (2H, dd, ^3J = 9.2 Hz, ^4J = 2.4 Hz), 6.24 (2H, d, ^4J = 2.4 Hz), 3.46 (8H, q, J = 7.3 Hz), 1.25 (12H, t, J = 7.3 Hz); ^{13}C NMR (75.5 MHz, DMSO-d_6) δ (ppm): 161.0, 159.9, 156.1, 143.6, 135.0, 121.8, 106.9, 96.7, 44.5, 12.5. ESI-HRMS: calcd for $C_{28}H_{33}B_2F_4N_4O_2$, 555.2730 (M + H), found 555.2704 (M + H). IR (ν, cm^{-1}): 1624.6, 1577.6, 1505.5, 1473.5, 1456.7, 1372.5, 1344.8, 1261.4, 1189.4, 1177.6, 1144.5, 1077.5, 1031.5, 968.0, 792.5, 783.6, 643.6, 531.8.

Polyboranil ***9***. General procedure II was followed leading to **9** as a yellow crystalline powder in 84% yield (102 mg). Mp: 240 °C. ^{1}H NMR (300 MHz, $CDCl_3$) δ (ppm): 7.93 (4H, m), 7.58 (4H, m), 7.23 (2H, d, ^3J = 9.3 Hz), 6.39 (2H, d, ^3J = 9.3. Hz), 6.32 (2H, s), 3.48 (8H, q, ^3J = 7,3 Hz), 1.27 (12H, t, ^3J = 7,3 Hz); ^{13}C NMR (75.5 MHz, $CDCl_3$) δ (ppm): 162.4, 156.7, 140.0, 134.3, 130.8, 126.6, 124.4, 123.8, 107.0, 106.3, 98.5, 45.5, 12.9. ESI-HRMS: calcd for $C_{32}H_{35}B_2F_4N_4O_2$, 605.2888 (M + H), found 605.2856 (M + H). IR (ν, cm^{-1}): 1620.1, 1591.1, 1502.4, 1447.0, 1402.4, 1345.0, 1233.4, 1142.0, 1071.6, 1035.7, 965.5, 784.1, 525.7.

Polyboranil ***10***. General procedure II was followed leading to **10** as a yellow amorphous powder in 63% yield (105 mg). ^{1}H NMR (300 MHz, $CDCl_3$) δ (ppm): 8.18 (3H, br s), 7.66 (3H, s), 7.37 (3H, d, ^3J = 8.8 Hz), 6.41 (3H, d, ^3J = 8.8 Hz), 6.23 (3H, s), 3.47 (12H, q, ^3J = 6.9 Hz), 1.26 (18H, t, ^3J = 6.9 Hz); ^{13}C NMR (75.5 MHz, $CDCl_3$) δ (ppm): 158.3, 157.8, 134.7, 116.5, 107.2, 98.0, 45.3, 12.7. ESI-HRMS: calcd for $C_{39}H_{45}B_3F_6KN_6O_3$, 831.3387 (M + K), found 831.3414 (M + K). IR (ν, cm^{-1}): 1622.3, 1575.2, 1504.6, 1455.8, 1417.0, 1343.7, 1260.9, 1175.6, 1142.1, 1071.7, 1031.8, 968.3, 889.2, 860.2, 820.9, 787.9, 715.7, 650.1, 526.2.

Polyboranil ***15***. General procedure II was followed leading to **15** as a red crystalline powder in 37% yield (44 mg). Mp: 292−293 °C. ^{1}H NMR (300 MHz, $CDCl_3$) δ (ppm) = 8.38 (br s, 2H), 7.81 (s, 1H), 6.76 (s, 1H), 6.74 (s, 4H), 3.90 (s, 12H), 3.89 (s, 6H). ^{13}C NMR (75 MHz, $CDCl_3$) δ (ppm) = 166.9, 161.1, 154.0, 140.0, 139.4, 137.9, 112.0, 107.7, 101.3, 92.9, 61.2, 56.6. ESI-HRMS: calcd for $C_{26}H_{26}B_2F_4KN_2O_8$, 631.1452 (M + K), found 631.1457 (M +K). IR (ν, cm^{-1}): 1635.8, 1597.4, 1579.1, 1464.8, 1410.9, 1337.8, 1224.9, 1172.9, 1122.8, 1033.2, 1013.1, 994.1, 931.0, 852.6, 834.6, 797.9, 648.0, 623.6.

Polyboranil ***16***. General procedure II was followed leading to **16** as a purple amorphous powder in 79% yield (105 mg). ^{1}H NMR (400 MHz, $CDCl_3$) δ (ppm) = 8.19 (s, 2H), 7.61 (s, 1H), 7.33 (d, 4H, ^3J = 8.8 Hz), 6.64 (s, 1H), 6.59 (d, 4H, ^3J = 8.8 Hz), 3.27 (t, 8H, ^3J = 7.2 Hz), 1.51−1.59 (m, 8H), 1.30−1.40 (m, 8H), 0.96 (t, 12H, ^3J = 7.6 Hz). ^{13}C NMR (75 MHz, $CDCl_3$) δ (ppm) = 165.3, 156.3, 148.8, 137.6, 129.6, 123.9, 112.1, 111.6, 106.9, 50.9, 29.3, 20.3, 14.0. ESI-HRMS: calcd for $C_{36}H_{49}B_2F_4N_4O_2$, 667.3984 (M + H), found 667.399. IR (ν, cm^{-1}): 1628.6, 1604.7, 1514.5, 1400.2, 1364.8, 1211.3, 1180.1, 1029.4, 954.6, 926.2, 893.1, 854.3, 807.6, 720.0, 532.8.

Polyboranil ***21***. General procedure II was followed, leading to **21** as a purple amorphous powder in 96% yield (128 mg). ^{1}H NMR (300 MHz, $CDCl_3$) δ (ppm) = 8.36 (br s, 2H), 7.55 (d, 4H, ^3J = 8.7 Hz), 7.06 (s, 2H), 6.69 (d, 4H, ^3J = 8.7 Hz), 3.36−3.31 (m, 8H), 1.63−1.58 (m, 8H), 1.42−1.34 (m, 8H), 0.98 (t, 12H, ^3J = 7.3 Hz). ^{13}C NMR (75 MHz, $CDCl_3$) δ (ppm) = 156.3, 150.2, 149.4, 129.9, 124.6, 122.8, 119.4, 111.8, 51.0, 29.3, 20.3, 14.0. ESI-HRMS: calcd for $C_{37}H_{48}B_2F_4N_4O_2$, 667.3984 (M + H), found 667.3970 (M + H). IR (ν, cm^{-1}): 1608.8, 1589.2, 1518.4, 1483.2, 1456.8, 1404.6, 1364.0, 1287.2, 1183.5, 1108.9, 1052.2, 925.7, 877.8, 813.3, 546.8.

General Procedure III for the Synthesis of Polyboranils 14 and 20. To a stirred solution of 0.2 mmol of the relevant polyanil **12** or **18** in 20 mL of distilled toluene was added BPh_3 (0.3 mmol, 1.5 equiv) as a powder. The resulting mixture was stirred at 90 °C, and the course of the reaction was monitored by TLC analysis. When the reaction was complete, it was allowed to cool. The solvent was removed in vacuo, and the residue was purified by silica gel chromatography using CH_2Cl_2 as eluent to yield polyboranils **14** or **20** as yellow powders (33−89% yield).

Polyboranil ***14***. General procedure III was followed, leading to **14** as a yellow amorphous powder in 33% yield (55 mg). ^{1}H NMR (300 MHz, $CDCl_3$) δ (ppm) = 8.16 (br s, 2H), 7.43−7.37 (m, 8H), 7.37 (s, 1H),7.26−7.19 (m, 12H), 6.62 (s, 1H), 6.15 (s, 4H), 3.80 (s, 6H), 3.54 (s, 12H). ^{13}C NMR (75 MHz, $CDCl_3$) δ (ppm) = 169.9, 160.4, 153.0, 141.1, 140.1, 138.1, 134.8, 133.5, 131.2, 128.1, 127.3, 126.9, 112.8, 107.7, 102.9, 61.1, 56.3. ESI-HRMS: calcd for $C_{50}H_{47}B_2N_2O_8$, 825.3529 (M + H), found 825.3514 (M + H). IR (ν, cm^{-1}): 1635.6, 1629.0, 1578.2, 1503.1, 1465.6, 1333.1, 1240.4, 1125.6, 1183.0, 1048.3, 1006.4.

Polyboranil ***20***. General procedure III was followed, leading to **20** as a yellow crystalline powder in 89% yield (151 mg). Mp: 275 °C dec. ^{1}H NMR (300 MHz, $CDCl_3$) δ (ppm) = 8.35 (s, 2H), 7.43−7.40 (m, 8H), 7.24−7.19 (m, 12H), 7.05 (s, 2H), 6.24 (s, 4H), 3.79 (s, 6H), 3.57 (s, 12H). ^{13}C NMR (75 MHz, $CDCl_3$) δ (ppm) = 162.3, 153.5, 153.0, 141.0, 138.6, 134.8, 133.7, 131.22, 129.8, 128.1, 127.3, 126.8, 125.7, 121.4, 121.0, 115.4, 102.7, 99.1, 61.1, 56.3. ESI-HRMS: calcd for $C_{50}H_{46}B_2N_2NaO_8$, 847.3332 (M+Na), found 847.3322 (M+Na). IR (ν, cm^{-1}): 1594.2, 1577.4, 1433.5, 1252.4, 1232.8, 1162.1, 1131.9, 1003.0, 988.3, 965.0, 840.8, 744.4, 730.7, 704.3, 688.2, 632.2, 619.2, 523.0.

■ ASSOCIATED CONTENT

Ⓢ Supporting Information

The Supporting Information is available free of charge on the ACS Publications website at DOI: 10.1021/acs.joc.6b01756.

^{1}H and ^{13}C spectra for all new compounds, HR-MS spectra, and spectroscopic and DLS data (PDF)

■ AUTHOR INFORMATION

Corresponding Authors

*E-mail: massue@unistra.fr.

*E-mail: gulrich@unistra.fr.

DOI: 10.1021/acs.joc.6b01756
J. Org. Chem. 2016, 81, 9658−9668

Notes

The authors declare no competing financial interest.

■ ACKNOWLEDGMENTS

J.M. and G.U. thank the Centre National de la Recherche Scientifique (CNRS) for funding, D.F. and K.B. thank the Ministère de l'Education Nationale, de la Recherche et de l'Enseignement Supérieur, for a Ph.D. grant, and M.M. thanks the Région Alsace and Amoneta Diagnostics for a Ph.D. grant.

■ REFERENCES

(1) (a) Beija, M.; Afonso, C. A. M.; Martinho, J. M. G. *Chem. Soc. Rev.* **2009**, *38*, 2410−2433. (b) Yan, Y.; Zhao, Y. S. *Chem. Soc. Rev.* **2014**, *43*, 4325−4340. (c) Liang, J.; Tang, B. Z.; Liu, B. *Chem. Soc. Rev.* **2015**, *44*, 2798−2811.

(2) (a) Yuan, L.; Lin, W.; Zheng, K.; He, L.; Huang, W. *Chem. Soc. Rev.* **2013**, *42*, 622−661. (b) Weil, T.; Vosch, T.; Hofkens, J.; Peneva, K.; Müllen, K. *Angew. Chem., Int. Ed.* **2010**, *49*, 9068−9093. (c) Kobayashi, H.; Ogawa, M.; Alford, R.; Choyke, P. L.; Urano, Y. *Chem. Rev.* **2010**, *110*, 2620−2640.

(3) (a) Climent, E.; Biyikal, M.; Gawlitza, K.; Dropa, T.; Urban, M.; Costero, A. M.; Martínez-Máñez, R.; Rurack, K. *Chem. - Eur. J.* **2016**, *22*, 11138−11142. (b) Lee, M. H.; Kim, J. S.; Sessler, J. *Chem. Soc. Rev.* **2015**, *44*, 4185−4191.

(4) (a) Mishra, A.; Bäuerle, P. *Angew. Chem., Int. Ed.* **2012**, *51* (9), 2020−2067. (b) Lin, Y.; Li, Y.; Zhan, X. *Chem. Soc. Rev.* **2012**, *41*, 4245−4272. (c) Hains, A. W.; Liang, Z.; Woodhouse, M. A.; Gregg, B. A. *Chem. Rev.* **2010**, *110*, 6689−6735.

(5) (a) Zhu, X.-H.; Peng, J.; Cao, Y.; Roncali, J. *Chem. Soc. Rev.* **2011**, *40*, 3509−3524. (b) Zhu, M.; Yang, C. *Chem. Soc. Rev.* **2013**, *42*, 4963−4976.

(6) (a) Loudet, A.; Burgess, K. *Chem. Rev.* **2007**, *107*, 4891−4932. (b) Ulrich, G.; Ziessel, R.; Harriman, A. *Angew. Chem., Int. Ed.* **2008**, *47*, 1184−1207. (c) Boens, N.; Leen, V.; Dehaen, W. *Chem. Soc. Rev.* **2012**, *41* (3), 1130−1172. (d) Lu, H.; Mack, J.; Yang, Y.; Shen, Z. *Chem. Soc. Rev.* **2014**, *43*, 4778−4823.

(7) Frath, D.; Massue, J.; Ulrich, G.; Ziessel, R. *Angew. Chem., Int. Ed.* **2014**, *53*, 2290−2310.

(8) (a) Massue, J.; Frath, D.; Ulrich, G.; Retailleau, P.; Ziessel, R. *Org. Lett.* **2012**, *14*, 230−233. (b) Massue, J.; Frath, D.; Retailleau, P.; Ulrich, G.; Ziessel, R. *Chem. - Eur. J.* **2013**, *19*, 5375−5386. (c) Benelhadj, K.; Massue, J.; Ulrich, G. *New J. Chem.* **2016**, *40*, 5877−5884. (d) Santra, M.; Moon, H.; Park, M.-H.; Lee, T.-W.; Kim, Y. K.; Ahn, K. H. *Chem. - Eur. J.* **2012**, *18*, 9886−9893. (e) Li, D.; Zhang, H.; Wang, C.; Huang, S.; Guo, J.; Wang, Y. *J. Mater. Chem.* **2012**, *22*, 4319−4328. (f) Kubota, Y.; Niwa, T.; Jin, J.; Funabiki, K.; Matsui, M. *Org. Lett.* **2015**, *17*, 3174−3177. (g) Kubota, Y.; Hara, H.; Tanaka, S.; Funabiki, K.; Matsui, M. *Org. Lett.* **2011**, *13*, 6544−6547.

(9) (a) Araneda, J. F.; Piers, W. E.; Heyne, B.; Parvez, M.; McDonald, R. *Angew. Chem., Int. Ed.* **2011**, *50*, 12214−12217. (b) Curiel, D.; Más-Montoya, M.; Usea, L.; Espinosa, A.; Orenes, R. A.; Molina, P. *Org. Lett.* **2012**, *14*, 3360−3363. (c) Frath, D.; Poirel, A.; Ulrich, G.; De Nicola, A.; Ziessel, R. *Chem. Commun.* **2013**, *49*, 4908−4910. (d) Fischer, G. M.; Daltrozzo, E.; Zumbusch, A. *Angew. Chem., Int. Ed.* **2011**, *50*, 1406−1409.

(10) (a) Baranov, M. S.; Lukyanov, K. A.; Borissova, A. O.; Shamir, J.; Kosenkov, D.; Slipchenko, L. V.; Tolbert, L. M.; Yampolsky, I. V.; Solntsev, K. M. *J. Am. Chem. Soc.* **2012**, *134*, 6025−6032. (b) Yoshino, J.; Kano, N.; Kawashima, T. *J. Org. Chem.* **2009**, *74*, 7496−7503. (c) Yoshino, J.; Kano, N.; Kawashima, T. *Chem. Commun.* **2007**, 559−561. (d) Pais, V. F.; Alcaide, M. M.; Lopez-Rodriguez, R.; Collado, D.; Najera, F.; Perez-Inestrosa, E.; Alvarez, E.; Lassaletta, J. M.; Fernandez, R.; Ros, A.; Pischel, U. *Chem. - Eur. J.* **2015**, *21*, 15369−15376.

(11) (a) Frath, D.; Azizi, S.; Retailleau, P.; Ulrich, G.; Ziessel, R. *Org. Lett.* **2011**, *13*, 3414−3417. (b) Grabarz, A. M.; Laurent, A. D.; Jędrzejewska, B.; Zakrzewska, A.; Jacquemin, D.; Ośmialowski, B. *J. Org. Chem.* **2016**, *81*, 2280−2292. (c) Benelhadj, K.; Massue, J.; Retailleau, P.; Chibani, S.; Le Guennic, B.; Jacquemin, D.; Ziessel, R.; Ulrich, G. *Eur. J. Org. Chem.* **2014**, *2014*, 7156−7164. (d) Wesela-Bauman, G.; Urban, M.; Lulinski, S.; Serwatowski, J.; Wozniak, K. *Org. Biomol. Chem.* **2015**, *13*, 3268−3279.

(12) Dobkowski, J.; Wnuk, P.; Buczynska, J.; Pszona, M.; Orzanowska, G.; Frath, D.; Ulrich, G.; Massue, J.; Mosquera-Vazquez, S.; Vauthey, E.; Radzewicz, C.; Ziessel, R.; Waluk, J. *Chem. - Eur. J.* **2015**, *21*, 1312−1327.

(13) (a) Song, P.; Chen, X.; Xiang, Y.; Huang, L.; Zhou, Z.; Wei, R.; Tong, A. *J. Mater. Chem.* **2011**, *21*, 13470−13475. (b) Feng, Q.; Li, Y.; Wang, L.; Li, C.; Wang, J.; Liu, Y.; Li, K.; Hou, H. *Chem. Commun.* **2016**, *52*, 3123−3126. (c) Wu, F.; Xu, G.; Zeng, X.; Mu, L.; Redshaw, C.; Wei, G. *J. Fluoresc.* **2015**, *25*, 1183−1189.

(14) (a) Tang, W.; Xiang, Y.; Tong, A. *J. Org. Chem.* **2009**, *74*, 2163−2166. (b) Chen, X.; Wei, R.; Xiang, Y.; Zhou, Z.; Li, K.; Song, P.; Tong, A. *J. Phys. Chem. C* **2011**, *115*, 14353−14359.

(15) (a) Hong, Y.; Lam, J. W. Y.; Tang, B. Z. *Chem. Commun.* **2009**, *29*, 4332−4353. (b) Mei, J.; Leung, N. L. C.; Kwok, R. T. K.; Lam, J. W. Y.; Tang, B. Z. *Chem. Rev.* **2015**, *115*, 11718−11940.

(16) Leung, N. L. C.; Xie, N.; Yuan, W.; Liu, Y.; Wu, Q.; Peng, Q.; Miao, Q.; Lam, J. W. Y.; Tang, B. Z. *Chem. - Eur. J.* **2014**, *20*, 15349−15353.

(17) Yan, L.; Zhang, Y.; Xu, B.; Tian, W. *Nanoscale* **2016**, *8*, 2471−2487.

(18) Frath, D.; Azizi, S.; Ulrich, G.; Ziessel, R. *Org. Lett.* **2012**, *14*, 4774−4777.

(19) (a) Li, D.; Zhang, Z.; Zhao, Y.; Wang, Y.; Zhang, H. *Dalton Trans* **2011**, *40*, 1279−1285. (b) Suresh, D.; Gomes, C. S. B.; Gomes, P. T.; Di Paolo, R. E.; Maçanita, A. L.; Calhorda, M. J.; Charas, A.; Morgado, J.; Duarte, M. T. *Dalton Trans* **2012**, *41*, 8502−8505. (c) Suresh, D.; Gomes, C. S. B.; Lopes, P. S.; Figueira, C. A.; Ferreira, B.; Gomes, P. T.; Di Paolo, R. E.; Maçanita, R. E.; Duarte, M. T.; Charas, A.; Morgado, J.; Vila-Viçosa, D.; Calhorda, M. J. *Chem. - Eur. J.* **2015**, *21*, 9133−9149.

(20) (a) Riddle, J. A.; Lathrop, S. P.; Bollinger, J. C.; Lee, D. *J. Am. Chem. Soc.* **2006**, *128*, 10986−10987. (b) Hou, Q.; Zhao, L.; Zhang, H.; Wang, Y.; Jiang, S. *J. Lumin.* **2007**, *126*, 447−451. (c) Dhanunjayarao, K.; Mukundam, V.; Ramesh, M.; Venkatasubbaiah, K. *Eur. J. Inorg. Chem.* **2014**, *2014*, 539−545. (d) Guieu, S.; Cardona, F.; Rocha, J.; Silva, A. M. S. *New J. Chem.* **2014**, *38*, 5411−5414.

(21) Hiremath, U. S. *Tetrahedron Lett.* **2013**, *54* (26), 3419−3423.

(22) Jeon, S.; Park, S.; Nam, J.; Kang, Y.; Kim, J.-M. *ACS Appl. Mater. Interfaces* **2016**, *8*, 1813−1818.

(23) Maury, O.; Viau, L.; Senechal, K.; Corre, B.; Guegan, J.-P.; Renouard, T.; Ledoux, I.; Zyss, J.; le Bozec, H. *Chem. - Eur. J.* **2004**, *10*, 4454−4466.

(24) Zakrzewska, A.; Kolehmainen, E.; Valkonen, A.; Haapaniemi, E.; Rissanen, K.; Chęcińska, L.; Ośmialowski, B. *J. Phys. Chem. A* **2013**, *117*, 252−256.

(25) Homocianu, M.; Airinei, A.; Dorohoi, D. O. *J. Adv. Res. Phys.* **2011**, *2*, 11105.

(26) Massue, J.; Retailleau, P.; Ulrich, G.; Ziessel, R. *New J. Chem.* **2013**, *37*, 1224−1230.

(27) (a) Loving, G. S.; Sainlos, M.; Imperiali, B. *Trends Biotechnol.* **2010**, *28*, 73−83. (b) Reichardt, C. *Chem. Rev.* **1994**, *94*, 2319−2358.

(28) Ośmialowski, B.; Zakrzewska, A.; Jędrzejewska, B.; Grabarz, A.; Zaleśny, R.; Bartkowiak, W.; Kolehmainen, E. *J. Org. Chem.* **2015**, *80*, 2072−2080.

(29) (a) Kato, S.-I.; Diederich, F. *Chem. Commun.* **2010**, *46*, 1994−2006. (b) Bures, F. *RSC Adv.* **2014**, *4*, 58826−58851.

(30) Shimizu, M.; Hiyama, T. *Chem. - Asian J.* **2010**, *5*, 1516−1531.

(31) (a) Brouwer, A. M. *Pure Appl. Chem.* **2011**, *83* (12), 2213−2228. (b) Würth, C.; Grabolle, M.; Pauli, J.; Spieles, M.; Resch-Genger, U. *Nat. Protoc.* **2013**, *8* (8), 1535−1550.

(32) Porrès, L.; Holland, A.; Pålsson, L.-O.; Monkman, A. P.; Kemp, C.; Beeby, A. *J. Fluoresc.* **2006**, *16* (2), 267−273.

(33) Castro-Osma, J. A.; North, M.; Wu, X. *Chem. - Eur. J.* **2016**, *22*, 2100−2107.

(34) Kumar, A.; Kumar, A.; Pandey, D. S. *Dalton trans.* **2016**, *45*, 8475−8484.

DOI: 10.1021/acs.joc.6b01756
J. Org. Chem. 2016, 81, 9658−9668

(35) A ^{13}C NMR spectrum was not obtained due to the inherent insolubility of **4** in $CDCl_3$ or DMSO at room temperature, 60 °C, or 80 °C.

DOI: 10.1021/acs.joc.6b01756
J. Org. Chem. 2016, 81, 9658−9668